Immune Determinants of the Association between Tumor Mutational Burden and Immunotherapy Response across Cancer Types

Neelam Sinha[1], Sanju Sinha[1], Cristina Valero[2,3], Alejandro A. Schäffer[1], Kenneth Aldape[4], Kevin Litchfield[5], Timothy A. Chan[6], Luc G.T. Morris[2,3], and Eytan Ruppin[1]

ABSTRACT

The FDA has recently approved a high tumor mutational burden (TMB-high) biomarker, defined by ≥10 mutations/Mb, for the treatment of solid tumors with pembrolizumab, an immune checkpoint inhibitor (ICI) that targets PD1. However, recent studies have shown that this TMB-high biomarker is only able to stratify ICI responders in a subset of cancer types, and the mechanisms underlying this observation have remained unknown. The tumor immune microenvironment (TME) may modulate the stratification power of TMB (termed TMB power), determining if it will be predictive of ICI response in a given cancer type. To systematically study this hypothesis, we inferred the levels of 31 immune-related factors characteristic of the TME of different cancer types in The Cancer Genome Atlas. Integration of this information with TMB and response data of 2,277 patients treated with anti-PD1 identified key immune factors that determine TMB power across 14 different cancer types. We find that high levels of M1 macrophages and low resting dendritic cells in the TME characterized cancer types with high TMB power. A model based on these two immune factors strongly predicted TMB power in a given cancer type during cross-validation and testing (Spearman Rho = 0.76 and 1, respectively). Using this model, we predicted the TMB power in nine additional cancer types, including rare cancers, for which TMB and ICI response data are not yet publicly available. Our analysis indicates that TMB-high may be highly predictive of ICI response in cervical squamous cell carcinoma, suggesting that such a study should be prioritized.

Significance: This study uncovers immune-related factors that may modulate the relationship between high tumor mutational burden and ICI response, which can help prioritize cancer types for clinical trials.

Introduction

Immunotherapy has shown remarkable clinical benefits in many cancers. However, its benefit is limited to a subset of patients, raising a need for response biomarkers (1). A frequently used biomarker is the tumor mutational burden (TMB), a measure of the total number of mutations in the coding regions of the genome (1, 2). The FDA has recently approved pembrolizumab, an immune checkpoint inhibitor (ICI) targeting PD1, for individuals with TMB-high (defined as ≥ 10 mutations/Mb) solid tumors (3). Despite this approval, the effectiveness of TMB-high as a biomarker for stratifying responders to immunotherapy, termed here TMB power, differs considerably across cancer types (4, 5), the mechanisms underlying these differences have remained unknown. Aiming to explain this clinically important finding, a previous report (6) has suggested that TMB-high may stratify IC blockade (ICB) responders in cancer types where TMB correlates with CD8 T-cell infiltration levels. This has pointed towards the potentially central role of the tumor microenvironment (TME) in determining this stratification power of TMB-high (termed TMB power). The TME, including $CD8^+$ T cells, dendritic cells, macrophages, B cells, T-cell receptor (TCR) repertoire, and major histocompatibility (MHC) locus status, has also been previously associated with the extent of immunotherapy response (1). Taking these studies into account, we hypothesized that differences in the immune activities in the TME of different cancer types may explain the variability observed in the TMB power across cancer types.

Materials and Methods

Data and preprocessing

All patients provided informed consent to an MSK Institutional Review Board–approved protocol, permitting the return of results from sequencing analyses for research. We collated: (i) a publicly available cohort of ICI-treated (anti–PD-1/PD-L1) patients' responses with TMB and demographic information, comprising 1,959 patients, and (ii) the data from an additional 318 patients, yielding a total of 2,277 patients across 14 cancer types. The clinical data do not distinguish whether a patient received anti–PD-1 or anti–PD-L1, so we analyzed these treatments together. The cancer types where all the patients have TMB < 10 Mutations/MB were excluded from our analysis. Sex is not used as a biological factor. No randomization or blinding is performed in this study. The Cancer Genome Atlas (TCGA; ref. 7) and MSKCC cohorts are publicly available cohorts

[1]Cancer Data Science Lab, Center for Cancer Research, National Cancer Institute, National Institute of Health, Bethesda, Maryland. [2]Department of Surgery, Memorial Sloan Kettering Cancer Center, New York, New York. [3]Immunogenomics and Precision Oncology Platform, Memorial Sloan Kettering Cancer Center, New York, New York. [4]Laboratory of Pathology, NCI, NIH, Bethesda, Maryland. [5]Cancer Evolution and Genome Instability Laboratory, The Francis Crick Institute, London, United Kingdom. [6]Center for Immunotherapy and Precision Immuno-Oncology, Cleveland Clinic, Lerner Research Institute, Cleveland Clinic, Cleveland, National Center for Regenerative Medicine, Cleveland Clinic, Cleveland, Ohio.

Note: Supplementary data for this article are available at Cancer Research Online (http://cancerres.aacrjournals.org/).

N. Sinha and S. Sinha contributed equally as co-first authors of this article.

Corresponding Author: Eytan Ruppin, NIH, 9000 Rockville Pike, Building 15C1, Bethesda, MD 20892. Phone: 240-858-3169; E-mail: eyruppin@gmail.com

Cancer Res 2022;82:2076–83

doi: 10.1158/0008-5472.CAN-21-2542

used in this study. We downloaded the mutation calls for the MSKCC from https://www.cbioportal.org/. We downloaded the omics data to compute immune-related factors levels in the TCGA (7) cohort from https://xenabrowser.net/datapages/?cohort=TCGA%20Pan-Cancer%20(PANCAN)&removeHub=https%3A%2F%2Fxena.treehouse.gi.ucsc.edu%3A443.

Computing TMB power for each cancer type

TMB power denotes the ability of TMB biomarkers to stratify responders versus nonresponders to anti–PD-1. We computed TMB power separately for three different forms of therapy response information: objective response rate (ORR), overall survival (OS), and progression-free survival (PFS). In the case of ORR, TMB power is defined as the odds ratio (OR) of response rate between TMB-high versus low group. If OS or PFS is available, we defined the TMB power as the ratio of death rate between TMB-high versus low group (1/hazard ratio (HR) of survival). Throughout the study, we report FDR-corrected *P* values.

Mean levels of immune factors across samples of a cancer type

These levels were mined from our previous publication (8) where a detailed methodology is provided. Please refer to the method section of ref. 8. To summarize, we classified immune-related factors into the following three types: (i) tumor neoantigen, (ii) tumor immune microenvironment, (iii) checkpoint target.

Tumor neoantigen

TMB was determined based on whole-exome sequencing (WES) data of TCGA samples. downloaded from UCSC Xena browser (https://xenabrowser.net/datapages/?dataset=GDC-PANCAN.somaticsniper_snv.tsv&host=https%3A%2F%2Fgdc.xenahubs.net&removeHub=https%3A%2F%2Fxena.treehouse.gi.ucsc.edu%3A443). TMB is defined as the total number of nonsynonymous single-nucleotide variants in each patient tumor. Intertumor heterogeneity was calculated using ABSOLUTE and the neoantigens were identified based on the neopeptides predicted to bind to MHC-I (https://gdc.cancer.gov/about-data/publications/panimmune).

Tumor immune microenvironment

Immune cell abundance was determined by applying a CIBERSORT (9). The cytolytic score is a measure of local immune cytolytic activity calculated by the geometric mean of gene expression of granzyme A (GZMA) and perforin (PRF1). TCR diversity was estimated from RNA sequencing (RNA-seq) using Shannon entropy and downloaded from the GDC pan-immune data portal (https://gdc.cancer.gov/about-data/publications/panimmune).

Checkpoint targets: PD-L1 expression

PD-L1 protein expression in each patient tumor was downloaded from the UCSC Xena browser (https://pancanatlas.xenahubs.net/download/TCGARPPA-pancan-clean.xena.gz).

We removed three immune factors, "active dendritic cells," "resting NK cells," and "active mast cell," from our initial set of 33 immune factors, due to low variance (0 in more than 50% of cancer types). In addition to these immune-related factors, we added sex ratio (Male to Female ratio) as a factor, to check the association between sex and TMB power (Total Immune Factors = 31).

Finding the immuno-modulators of TMB power

The correlation between TMB power and the mean level of 31 immune-related factors was calculated. We ranked the modulators by the correlation between their mean levels and TMB power across cancer types in three different analyses: (i) We considered three different measures of outcomes (OS, PFS, ORR) to compute TMB power, (ii) We considered the correlations obtained both across all cancer types and those obtained considering only cancer types with significant HR/OR ratios, and finally, (iii) We measured both Pearson and Spearman correlations. We computed an average rank across these analyses and decided to focus and highlight the top and bottom two ranked modulators based on the correlation strength. We considered both Pearson and Spearman correlations, as both methods have limitations. The former is susceptible to outliers and the latter does not take into account the effect size.

Multivariate regression model to predict TMB power

We next built a multivariate linear regression model based on the above four modulators, using a standard leave-one-out cross-validation method. Here, we built a model using all possible combinations of features exhaustively and the performance of the prediction was evaluated based on Spearman rank correlation (rho). Using the best model, we next predicted TMB power for 17 additional cancer types where it is unknown. Among these, we noted that feature values are in the interpolation range, i.e., the range on which our model was trained, for only 9 of 17 cancer types and thus we restricted our prediction for these cancer types.

Data availability

The study's scripts and data are provided to replicate each step of results and plots in GitHub repository: https://github.com/ruppinlab/Immune_determinant_for_power_of_TMB. We also generated and provided a standard and executable research package at the codeocean: https://codeocean.com/capsule/7166680. Genomic and clinical data from the MSK-IMPACT cohort used for these analyses are available as Supplementary Table S1. Requests for additional data from this cohort should be directed to either the corresponding author or Luc Morris per MSK's clinical and genomic data sharing policies.

Results

To study this hypothesis, we first collated the largest publicly available cohort of ICI-treated (anti-PD1/anti-PDL1) patient's responses with TMB and demographic information (Supplementary Table S2), comprising 1,959 patients (4, 5, 10, 11) together with an additional new cohort of 318 patients, comprising a total of 2,277 patients across 14 cancer types (Supplementary Table S1, includes patient ages). Analyzing this combined cohort, we first aimed to depict the association between TMB-high and patients' response to ICI in each cancer type. To this end, we computed the difference in OS between patients with high TMB versus low TMB, i.e., the HR of survival, in each cancer type (**Fig. 1A**). The HR is significantly < 1 for 8 of 14 cancer types (using FDR < 0.1 as a significance threshold), testifying to overall higher survival in patients with TMB-high, however, its magnitude varies considerably across cancer types. In pancreatic adenocarcinoma (PAAD), the HR is significantly greater than 1 (FDR < 0.1) presenting evidence against the usage of the TMB-high biomarker to select patients. A similar trend and variability are observed for PFS (Supplementary Fig. S1). Repeating this analysis using the tumor response status and computing the OR of ORR, the radiological assessment of the tumor burden after treatment, between TMB-high versus low TMB patients, 5 of 11 cancer types have a significant OR > 1 (FDR < 0.1; **Fig. 1B**), testifying to a higher response

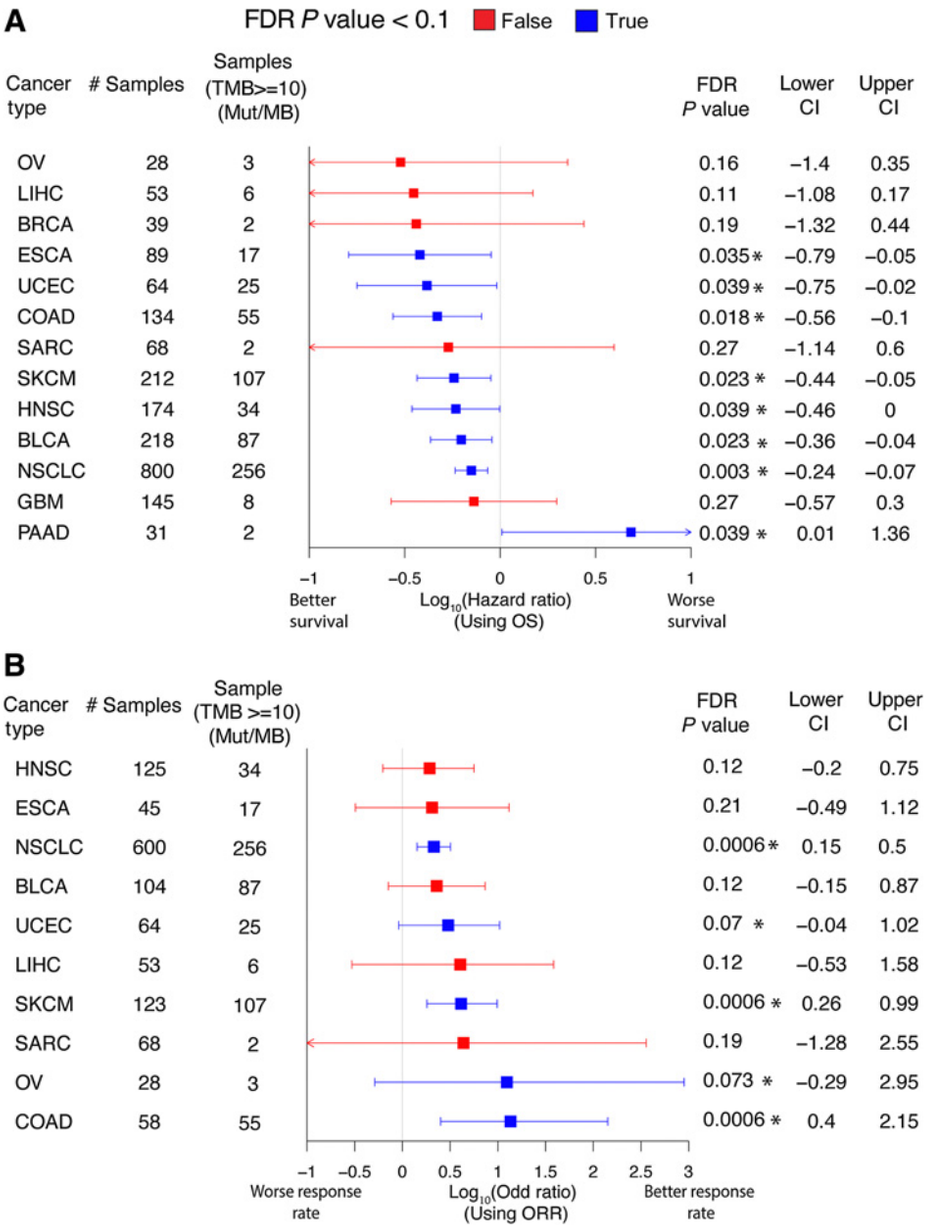

Figure 1.

ICI response of TMB-high versus TMB low groups for different cancer types. **A,** HR of OS (*x*-axis) between patients with high versus low TMB computed using a Cox regression model. Cancer types having a significant HR are colored blue versus red, denoting cancer types for which the HR is not significant. Error bars represent the 95% confidence interval (CI) and *P* values were computed using a log-rank test. Cancer type abbreviations follow those used in TCGA (7). The number of patients with each cancer type is provided in the second column. The number of patients in the High TMB group (for each cancer type) is provided in the third column. **B,** The results of a similar analysis using response status and the OR. Renal cell carcinoma (KIRC) is not reported in **A**, as its HR cannot be computed confidently. FDR corrected *P* value is provided in the 5th column; the 6th and 7th columns represent the CI range.

rate in patients with TMB-high, but not in all cancer types. These observations are in line with previous findings (4, 5), showing that the TMB-high biomarker based on a universal FDA-approved cutoff is predictive of response only in a subset of cancer types, with variable predictive power. We quantify the stratification power of TMB in identifying immunotherapy responders (termed TMB power) in each cancer type as 1/HR in terms of OS or PFS and OR in terms of tumor response.

We next quantified the mean levels of various immune-related factors in the TME of a given cancer type. To this end, we mined WES and RNA-seq data of pretreated samples for the above 14 cancer types from TCGA. In each cancer type, we estimated the mean levels of 31 different immune-related factors (Supplementary Table S3) which have been previously reported to be associated with ICI response (8). Those include (i) tumor neoantigen characteristics, including neoantigen hydrophobicity, intratumor heterogeneity, and neoantigen burden; (ii) TME characteristics, including the abundance of different immune cells, the cytolytic score, T-cell exhaustion, and IFNγ signatures, and TCR diversity, and finally, (iii) checkpoint target–related variables, including PD-L1 protein expression, the combined positive score (defined as the ratio of the number of PD-L1 staining cells (tumor cells, lymphocytes, macrophages) out of the total number of viable cells) and fPD1 (the fraction of high PD1 staining tumors in a given cancer type).

To identify the immune-related modulators of TMB power, we computed the correlation between the mean levels of each immune factor described above and the three measures of TMB power based on OS, ORR, and PFS, across the 14 cancer types we studied (**Fig. 2A** and **B**; Supplementary Fig. S2A leftmost, in respective order). Four immune factors emerge as being correlated with the TMB power

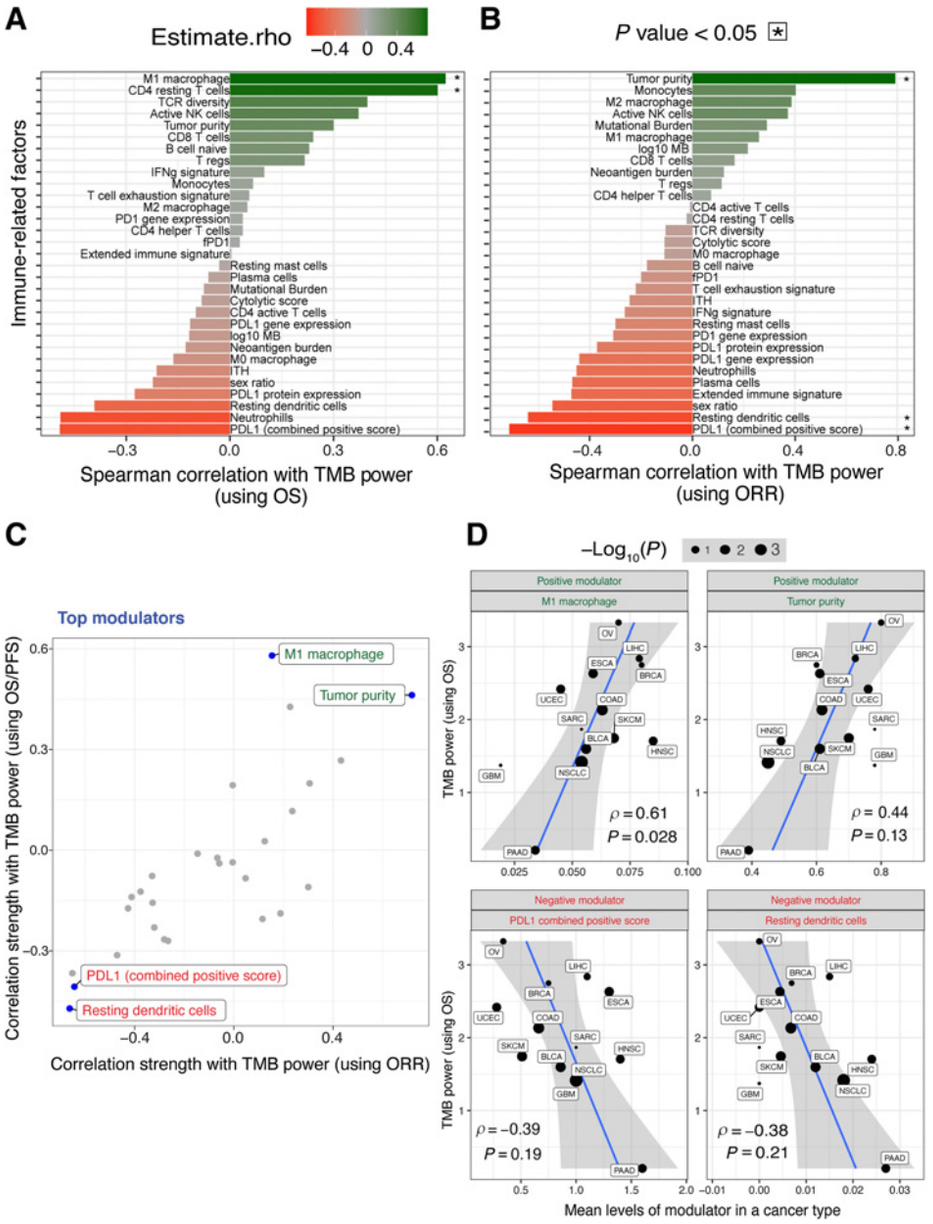

Figure 2.

Immune modulators of TMB power. **A,** Correlation strength between TMB power based on OS and levels of immune-related factors across 14 cancer types, computed using Spearman Rho (x-axis). Green and red bars denote positive and negative modulators, respectively, and the intensity of the color denotes the strength of correlation. Significant correlations, *, $P < 0.05$, and four highly correlated modulators are shown in bold. **B,** This analysis is repeated to identify modulators of TMB power based on tumor response status (ORR). **C,** The strength of correlation with TMB power using ORR (*x*-axis) and OS/PFS (*y*-axis) is provided for each modulator, where the top four are highlighted and labeled. The *y*-axis is the mean correlation strength of each modulator level with TMB power when OS and PFS are used across two cases—when all cancer types are used and when only cancer types with significant TMB power are used. **D,** Scatter plots show the relationship between the mean levels of each of the four top modifiers in a cancer type (*x*-axis) and the TMB power (in terms of OS). The best fit line is provided in blue, where the shaded region denotes a 95% confidence interval. Renal cell carcinoma (KIRC) is not reported in **D**, as its HR cannot be computed confidently.

for all three outcomes measures (**Fig. 2C**). Two modulators are positively correlated with the TMB power, including M1 macrophage levels (correlation strength with TMB power based on OS is Spearman $\rho = 0.61$, $P = 0.02$; **Fig. 2D**, top left) and tumor purity levels (Spearman $\rho = 0.44$, $P = 0.13$; **Fig. 2D**, top right). We termed them positive modulators. Two other modulators are negatively correlated with the TMB power (negative modulators), including the PDL1 combined positive score (Spearman $\rho = -0.39$, $P = 0.19$; **Fig. 2D**-bottom-left) and resting dendritic cells (Spearman Rho $= -0.38$, $P = 0.21$; **Fig. 2D**-bottom right). We note that the overall level of lymphocytes is not significantly associated with TMB power.

Repeating the above analysis using only cancer types with statistically significant HRs or ORs (Materials and Methods) yielded concordant findings, where the same four modulators are the top-ranked (Supplementary Fig. S2B and S2C). We next aimed to validate our top modulators in independent ICB cohorts. The largest publicly available cohort (12) has three cancer types (HNSC, head and neck squamous cell carcinoma; NSCLC; non-small cell lung cancer; SKCM, skin cutaneous melanoma) that can be analyzed to further test and validate the robustness of the top modulators identified on the basis of the MSKCC data (Supplementary Table S4). To perform this analysis, we merged the suitable data, overall comprising 341 patients (treated with anti–PD-1), with our initial MSKCC dataset and repeated with analysis. Reassuringly, we find that each of our top four modulators remains robustly top-ranked (Supplementary Fig. S3).

We next built a multivariate linear model predicting TMB power at a given cancer type based on the levels of the four top modulators identified above, assessing their aggregate predictive power in a leave-one-out cross-validation procedure. We built this model separately for all three measures of TMB power (OS, PFS, ORR). The models

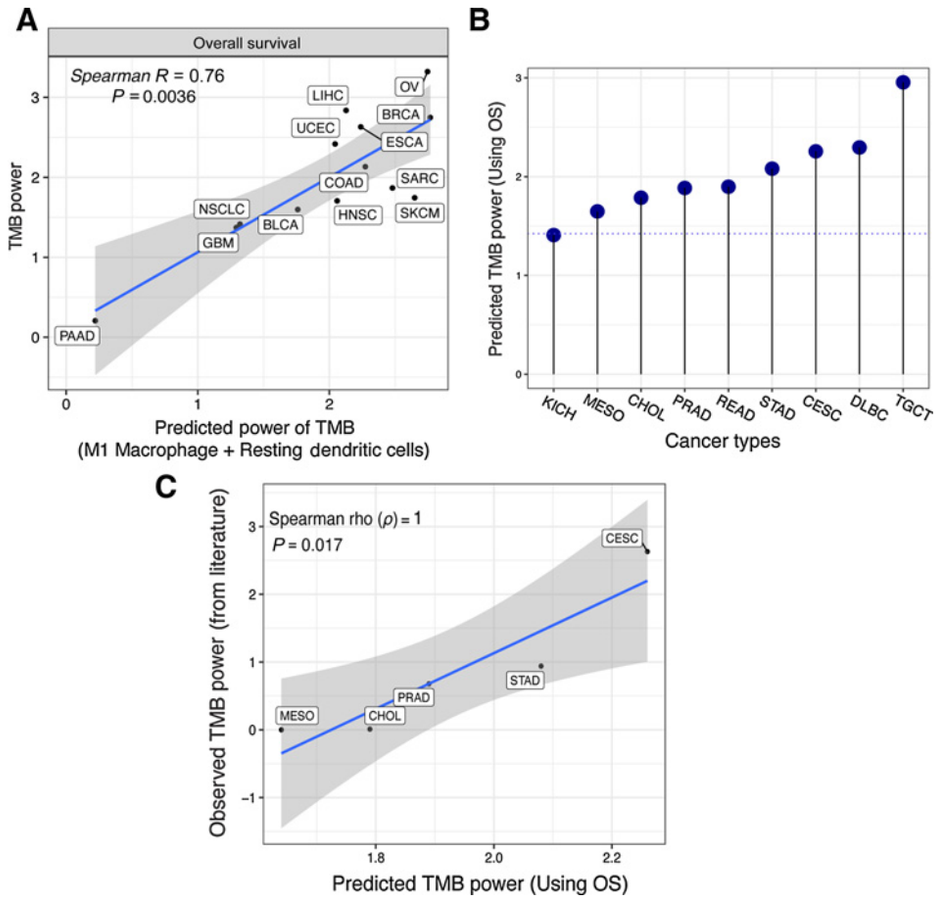

Figure 3.
Predicting TMB power across cancer types. **A,** The correlation between observed TMB power (*y*-axis) and its predicted value is based on M1 macrophage and resting dendritic cell levels. The best fit line is provided in blue, where the shaded region denotes the 95% confidence interval. The Spearman correlation and significance are provided at the left top corner. **B,** Predicted TMB power using this model (*y*-axis) in 9 additional cancer types (*x*-axis), the blue dotted horizontal line shows the TMB power observed for NSCLC. **C,** The correlation between observed TMB power from the literature (*y*-axis) and its predicted value. The Spearman correlation and significance are provided at the left top corner.

performing best TMB power computed using durable survival only used two features, M1 macrophage and resting dendritic cells levels predicting TMB power based on OS with a Spearman $\rho = 0.76$, $P = 0.0036$ (**Fig. 3A**; Supplementary Table S5). Adding the two remaining modulators does significantly not improve model performance. We note that liver hepatocellular carcinoma (LIHC) and SKCM are the cancer types where the immune modulators are not well able to predict the TMB power compared with the rest of the cancer types.

Using this two-feature linear model, we predicted the TMB power in 17 additional cancer types. These cancer types do not have publicly available TMB and ICI response data but their mean levels of M1 macrophage and resting dendritic cells could still of course be estimated from the TCGA cohort. We could confidently predict TMB power for 9 of these cancer types, where the two modulators' levels were within the interpolation range of the regression (Materials and Methods). Notably, in 8 of these, the predicted TMB power was greater than that observed for lung cancer, where TMB-high patients have been shown to have a higher response rate and median survival in large clinical trials (**Fig. 3B**; Supplementary Table S6; ref. 13). The top-ranked cancer types are TGCT (testicular germ cell tumors, TMB power = 2.95, two times higher than the TMB power observed in lung cancer), DLBC (lymphoid neoplasm diffuse large B-cell lymphoma, TMB power = 2.30, 1.6 times higher than the TMB power observed for lung cancer) and CESC (cervical squamous cell carcinoma, TMB power = 2.26, 1.6 times higher than the TMB power observed for lung cancer). Among those, we think that cervical squamous cell carcinoma is probably the most interesting cancer type to further test the utility of TMB-high as a biomarker, as it has the highest overall immunotherapy response rate [20%, mined from (8)]. The distributions of the most significant modulators are plotted in Supplementary Fig. S4.

Testing these TMB power predictions, we performed a literature survey of all the immunotherapy clinical trials with TMB and response data of these nine cancer types. We were able to find such trials for five out of nine cancer types (MESO, CHOL, PRAD, STAD, CESC) and computed their observed TMB power. The correlation between the TMB power predicted via our model and the one observed in the literature is significant (Spearman Correlation = 1, $P = 0.017$; **Fig. 3C**; and Pearson correlation = 0.93, $P = 0.02$). This testifies to the model's ability to order cancer types by the extent to which the model can predict their TMB power.

We next compared our model performance to the only previous published attempt to predict the TMB power (6). Their model is based on a single feature - the strength of correlation between the CD8 T-cells abundance and neoantigen burden in a cancer type (termed as the Neoantigen-CD8 correlation strength in our analysis). We first observed that the Neoantigen-CD8 correlation strength is not significantly correlated with TMB power computed using either OS, PFS, or ORR (Supplementary Fig. S5A–S5C) and the rank of our four modulators is higher than the Neoantigen-CD8 correlation strength in all these cases (Supplementary Fig. S5D). Testing their model on our data, we observed that the predictive performance of McGrail and colleagues's model is markedly lower than that of our model (it

achieves Spearman correlations between predicted and observed TMB power based on OS, ORR, and PFS of 0.07, 0.18, and −0.09, respectively, which are an order of magnitude lower than that of our model Supplementary Fig. S5E and S5F)." Furthermore, our model also showed better performance in a test set of five additional cancer types that are not used to build our model (Performances of our model and McGrail and colleague's model in Spearman Rho are 1 versus 0.7, respectively and Pearson correlation are 0.93 versus 0.6).

Testing the robustness of our top modulators

We next test the robustness of our top modulators by repeating the identification process in a series of different contexts including (i) removing outliers, (ii) a different high-TMB cutoff, and (iii) only considering the same stage and patient sex distribution in both cohorts. We first repeated our analysis removing PAAD, an outlier in **Fig. 2D**, and observed concordant findings (**Fig. 4A**; Supplementary Fig. S6), We next repeated our analysis considering the top 20% percentile of patients as high-TMB and found that 3 of 4 of our top modulators are still among top-ranked (**Fig. 4B**; Supplementary Fig. S7). We next repeated our analysis by only considering TCGA patients' metastatic disease with the same proportion as that reported for the MSKCC cohort to consider comparable ICB-treated patients' disease stage in the two cohorts, MSKCC and TCGA (with same patients' sex distribution as well). We first note an overall consistent rank of all the modulators compared to the initial ranking (Spearman Rho = 0.44, $P < 0.08$). Among the two of our initial top modulators that can be computed in this cohort, our top negative modulator identified in the original analysis, the resting dendritic cell is among the top ones (rank = 2nd; **Fig. 4C**; Supplementary Fig. S8).

Going beyond cancer types-levels, we next tested whether, within a cancer type, our modulators can stratify subgroups of patients' where high-TMB would be predictive of ICB response in four different cohorts (12, 14–17). We find that the predictive power of our modulators identified across cancer types does not translate to stratifying subgroups of patients that have distinct TMB power within a cancer type (**Fig. 4D–F**). Thus, the predictive power of the modulators of TMB power is quite analogous to that of TMB-high levels themselves, which while it is a strong determinant of response to immunotherapy across different cancer types, it is a much weaker determinant of response of individual patients within a given cancer type (18, 19).

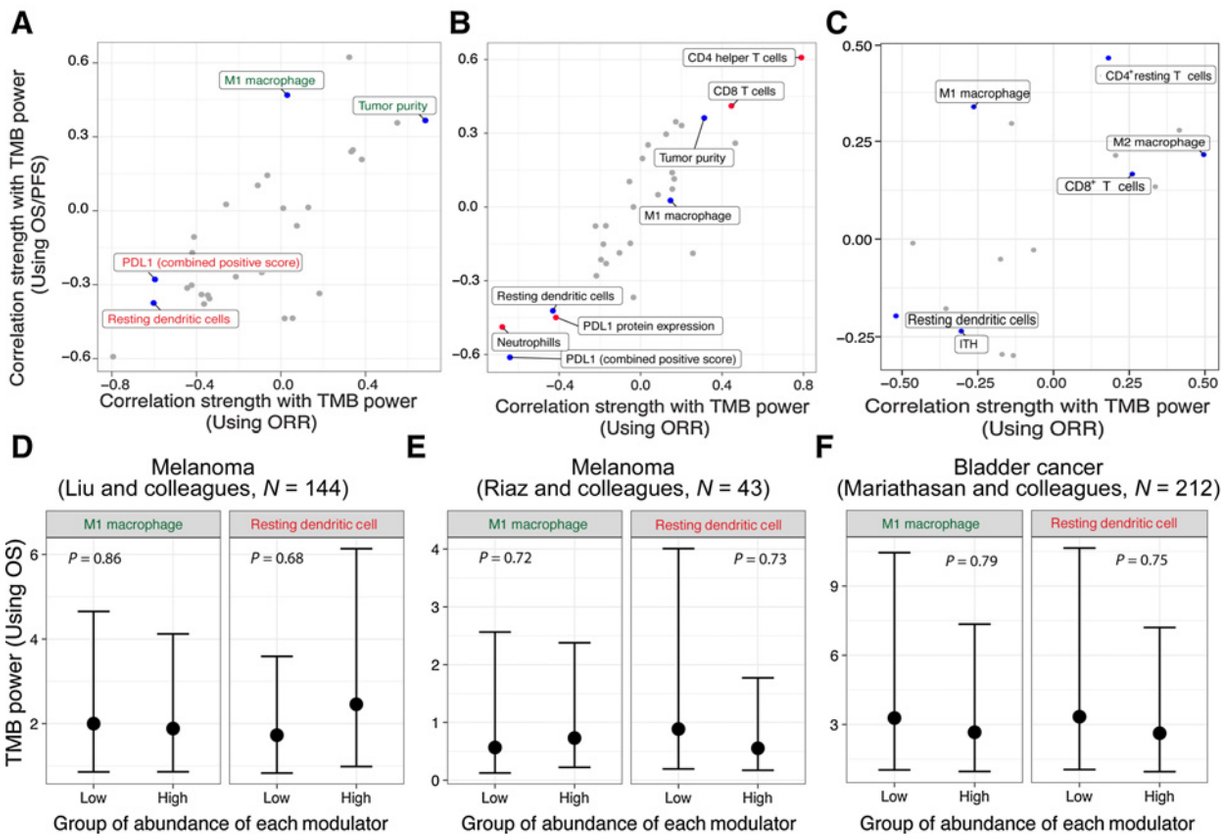

Figure 4.

Testing the robustness of top modulators in different contexts. **A,** The strength of correlation with TMB power using ORR (*x*-axis) and OS/PFS (*y*-axis) is provided for each modulator, where the green text (highlighted and labeled) represent the positive modulators identified using our initial pipeline and the red text (highlighted and labeled) represents the negative modulators when we repeat the analysis after removing outliers (pancreatic cancer). **B** and **C,** Shows the results when repeating the analysis using different cut-off points of TMB-high (TMB-high ≥ 20 percentile) in each cancer type (**B**), and similarly, when the analysis is repeated after only considering the same stage and patient's sex distributions in both cohorts (**C**). **D–F,** The difference in TMB power between subgroups within a cancer type based on high versus low levels (top vs. bottom 50% quantile) of the top modulators: M1 macrophage and resting dendritic cell, in melanoma, Liu and colleagues (**D**; ref. 14), melanoma, Riaz and colleagues (**E**; ref. 15), and bladder cancer, Mariathasan and colleagues (**F**; ref. 16). The TMB power is not shown for a melanoma, Hugo and colleagues (17), as the Cox regression did not converge.

Discussion

We identified two key immune-related factors whose levels are associated with the ability of TMB-high biomarkers to stratify immunotherapy responders. Specifically, we find that high levels of M1 macrophages and low resting dendritic cells are predictive of cancer types with high *TMB* power. Aligned with these findings, M1 macrophages have been reported to provide an antitumor environment by fostering an inflammation response against tumor activating CD8 T cells, and thus their higher levels would likely augment the response to immunotherapy (20). In contrast, resting dendritic cells provide a protumor environment by inducing tolerance to tumor antigens via inducing T cell death or an anergic state (long-term inactivated state) or suboptimal priming, and thus their higher levels would likely suppress the response to immunotherapy (21, 22). Our approach leverages existing data to (i) prioritize cancer indications for trials that investigate whether TMB is an effective biomarker in a new, yet unexplored or under-explored, cancer types (ii) how TMB might be combined with other variables to arrive at a more predictive biomarker of this latter task.

One limitation of our study is that our analysis is based on immune factors computed by deconvolution of bulk tumor data, which even though now being an accepted practice employed in many studies, only reflects estimations of different cell populations in the TME. Second, we should note that our analysis combined data on patients receiving different formulations of anti-PD1 and anti-PDL1 (aiming to increase the statistical power of the analysis), whereas the FDA has approved to date, only the usage of a high-TMB biomarker for the treatment of pembrolizumab, a specific anti-PD1. Consequently, we expect that our results would be further refined as single cell-based measurements of immune cells abundance and activity in different cancer types are computed, including the application of recently developed expression deconvolution software tools to obtain a better estimation of TME immune factors in each cancer type (9, 23).

We note that the three related measures of mutation counts, log10 (MB), mutational burden, and neoantigen burden are correlated. While two of these pairs are strongly correlated but not entirely so (Spearman correlation between log10 MB and Mutational Burden: 0.81, log10 MB, and Neoantigen Burden: 0.79), the correlation between Mutational Burden and Neoantigen Burden is indeed almost perfect (Spearman Rho = 0.99).

Authors' Disclosures

S. Sinha reports other support from NCI-UMD Partnership for Integrative Cancer Research Program during the conduct of the study. C. Valero reports grants from Fundación Alfonso Martín Escudero and grants from NIH - Cancer Center Support Grant P30 CA008748 during the conduct of the study. K. Litchfield reports personal fees from Roche Tissue Diagnostics; grants from CRUK TDL/Ono/LifeArc alliance; and personal fees from Monopteros Therapeutics outside the submitted work; in addition, K. Litchfield has a patent for Indel burden and CPI response pending. T.A. Chan reports grants from PGDx, Pfizer, Varian; grants and personal fees from Illumina, Nysnobio; and grants and personal fees from AstraZeneca during the conduct of the study; in addition, T.A. Chan has a patent for Use of TMB as biomarker pending. L. Morris reports a patent for Application US 2019/0092864/A1 pending to PGDx. No disclosures were reported by the other authors.

Authors' Contributions

N. Sinha: Conceptualization, data curation, software, formal analysis, validation, visualization, methodology, writing–original draft, project administration, writing–review and editing. **S. Sinha:** Conceptualization, data curation, software, formal analysis, supervision, validation, visualization, methodology, writing–original draft, project administration. **C. Valero:** Resources, writing–original draft. **A.A. Schäffer:** Formal analysis, supervision, writing–original draft. **K. Aldape:** Writing–original draft. **K. Litchfield:** Resources. **T.A. Chan:** Resources. **L.G.T. Morris:** Resources, writing–review and editing. **E. Ruppin:** Conceptualization, supervision, writing–original draft, project administration, writing–review and editing.

Acknowledgments

This research used the computational resources of the NIH HPC Biowulf cluster (http://hpc.nih.gov). This research was supported by the Intramural Research Program of the NIH, NCI, by Fundación Alfonso Martín Escudero (to C. Valero) and the NIH Cancer Center Support Grant P30 CA008748. S. Sinha is supported by the NCI-UMD Partnership for Integrative Cancer Research Program. L.G.T. Morris is supported by the NIH R01 DE027738 grant.

Received August 4, 2021; revised December 12, 2021; accepted April 1, 2022; published first April 6, 2022.

References

1. Jardim DL, Goodman A, de Melo Gagliato D, Kurzrock R. The challenges of tumor mutational burden as an immunotherapy biomarker. Cancer Cell 2021; 39:154–73.
2. Marabelle A, Fakih M, Lopez J, Shah M, Shapira-Frommer R, Nakagawa K, et al. Association of tumor mutational burden with outcomes in patients with advanced solid tumors treated with pembrolizumab: prospective biomarker analysis of the multicohort, open-label, phase II KEYNOTE-158 study. Lancet Oncol 2020;21:1353–65.
3. U.S. Food and Drug Administration. FDA approves pembrolizumab for adults and children with TMB-H solid tumors. News release. FDA. June 17, 2020. Available from: https://bit.ly/30QEt40.
4. Samstein RM, Lee CH, Shoushtari AN, Hellmann MD, Shen R, Janjigian YY, et al. Tumor mutational load predicts survival after immunotherapy across multiple cancer types. Nat Genet 2019;51:202–6.
5. Valero C, Lee M, Hoen D, Zehir A, Berger MF, Seshan VE, et al. Response rates to anti–PD-1 immunotherapy in microsatellite-stable solid tumors with 10 or more mutations per megabase. JAMA Oncol 2021;75: 739–43.
6. McGrail DJ, Pilié PG, Rashid NU, Voorwerk L, Slagter M, Kok M, et al. High tumor mutation burden fails to predict immune checkpoint blockade response across all cancer types. Ann Oncol 2021;32:661–72.
7. Hoadley KA, Yau C, Hinoue T, Wolf DM, Lazar AJ, Drill E, et al. Cell-of-origin patterns dominate the molecular classification of 10,000 tumors from 33 types of cancer. Cell 2018;173:291–304.
8. Lee JS, Ruppin E. Multiomics prediction of response rates to therapies to inhibit programmed cell death 1 and programmed cell death 1 ligand 1. JAMA Oncol 2019;5:1614–8.
9. Newman AM, Steen CB, Liu CL, Gentles AJ, Chaudhuri AA, Scherer F, et al. Determining cell type abundance and expression from bulk tissues with digital cytometry. Nat Biotechnol 2019;37:773–82.
10. Valero C, Lee M, Hoen D, Weiss K, Kelly DW, Adusumilli PS, et al. Pretreatment neutrophil-to-lymphocyte ratio and mutational burden as biomarkers of tumor response to immune checkpoint inhibitors. Nat Comm 2021;12:729.
11. Valero C, Lee M, Hoen D, Wang J, Nadeem Z, Patel N, et al. The association between tumor mutational burden and prognosis is dependent on treatment context. Nat Genet 2021;53:11–15.
12. Litchfield K, Reading JL, Puttick C, Thakkar K, Abbosh C, Bentham R, et al. Meta-analysis of tumor- and T-cell–intrinsic mechanisms of sensitization to checkpoint inhibition. Cell 2021;184:596–614.
13. Chan TA, Yarchoan M, Jaffee E, Swanton C, Quezada SA, Stenzinger A, et al. Development of tumor mutation burden as an immunotherapy biomarker: utility for the oncology clinic. Ann Oncol 2019;30:44–56.
14. Liu D, Schilling B, Liu D, Sucker A, Livingstone E, Jerby-Arnon L, et al. Integrative molecular and clinical modeling of clinical outcomes to PD1 blockade in patients with metastatic melanoma. Nat Med 2019;25:1916–27.
15. Riaz N, Havel JJ, Makarov V, Desrichard A, Urba WJ, Sims JS, et al. Tumor and microenvironment evolution during immunotherapy with nivolumab. Cell 2017;171:934–49.

16. Mariathasan S, Turley SJ, Nickles D, Castiglioni A, Yuen K, Wang Y, et al. TGFβ attenuates tumor response to PD-L1 blockade by contributing to exclusion of T cells. Nature 2018;554:544–8.
17. Hugo W, Zaretsky JM, Sun L, Song C, Moreno BH, Hu-Lieskovan S, et al. Genomic and transcriptomic features of response to anti–PD-1 therapy in metastatic melanoma. Cell 2016;165:35–44.
18. Yarchoan M, Hopkins A, Jaffee EM. Tumor mutational burden and response rate to PD-1 inhibition. N Engl J Med 2017;377:2500–1.
19. Jing Y, Liu J, Ye Y, Pan L, Deng H, Wang Y, et al. Multi-omics prediction of immune-related adverse events during checkpoint immunotherapy. Nat Commun 2020;11:4946.
20. Lin Y, Xu J, Lan H. Tumor-associated macrophages in tumor metastasis: biological roles and clinical therapeutic applications. J Hematol Oncol 2019;12:76.
21. Joffre O, Nolte MA, Spörri R, Reis e Sousa C. Inflammatory signals in dendritic cell activation and the induction of adaptive immunity. Immunol Rev 2009;227:234–47.
22. Fu C, Jiang A. Dendritic cells and CD8 T-cell immunity in tumor microenvironment. Front Immunol 2018;9:3059.
23. Wang K, Patkar S, Lee JS, Michael Gertz E, Robinson W, Schischlik F, et al. Deconvolving clinically relevant cellular immune crosstalk from bulk gene expression using CODEFACS and LIRICS stratifies melanoma patients to anti–PD-1 therapy. Cancer Discov 2022;12:1088–105.